An analytical solution for McIntyre's model of avalanche triggering probability for SPAD compact modeling and performance exploration

Tulio Chaves de Albuquerque, Dylan Issartel, Shaochen Gao, Younes Benhammou, Dominique Golanski, Raphaël Clerc, Calmon F.

▶ **To cite this version:**

Tulio Chaves de Albuquerque, Dylan Issartel, Shaochen Gao, Younes Benhammou, Dominique Golanski, et al.. An analytical solution for McIntyre's model of avalanche triggering probability for SPAD compact modeling and performance exploration. Semiconductor Science and Technology, 2021, 10.1088/1361-6641/ac00d0 . hal-03255595

HAL Id: hal-03255595
https://hal.science/hal-03255595v1

Submitted on 4 Dec 2024

HAL is a multi-disciplinary open access archive for the deposit and dissemination of scientific research documents, whether they are published or not. The documents may come from teaching and research institutions in France or abroad, or from public or private research centers.

L'archive ouverte pluridisciplinaire **HAL**, est destinée au dépôt et à la diffusion de documents scientifiques de niveau recherche, publiés ou non, émanant des établissements d'enseignement et de recherche français ou étrangers, des laboratoires publics ou privés.

Semiconductor Science and Technology

PURPOSE-LED PUBLISHING™

PAPER • **OPEN ACCESS**

An analytical solution for McIntyre's model of avalanche triggering probability for SPAD compact modeling and performance exploration

To cite this article: Tulio Chaves De Albuquerque *et al* 2021 *Semicond. Sci. Technol.* **36** 085008

View the article online for updates and enhancements.

You may also like

- Recent advances in InGaAs/InP single-photon detectors
Chao Yu, Qi Xu and Jun Zhang
- High photon detection efficiency InGaAs/InP single photon avalanche diode at 250 K
Tingting He, Xiaohong Yang, Yongsheng Tang et al.
- Impact of silicide layer on single photon avalanche diodes in a 130 nm CMOS process
Zeng Cheng, Darek Palubiak, Xiaoqing Zheng et al.

This content was downloaded from IP address 134.214.16.237 on 04/12/2024 at 08:36

OPEN ACCESS
IOP Publishing
Semiconductor Science and Technology
Semicond. Sci. Technol. **36** (2021) 085008 (8pp)
https://doi.org/10.1088/1361-6641/ac00d0

An analytical solution for McIntyre's model of avalanche triggering probability for SPAD compact modeling and performance exploration

Tulio Chaves De Albuquerque[1,2], Dylan Issartel[1], Shaochen Gao[1], Younes Benhammou[1,2], Dominique Golanski[2], Raphaël Clerc[3] and Francis Calmon[1,*]

[1] Univ Lyon, INSA Lyon, CNRS, Ecole Centrale de Lyon, Université Claude Bernard Lyon 1, CPE Lyon, INL, UMR5270, Villeurbanne, France
[2] STMicroelectronics, Crolles, France
[3] Univ Jean Monnet de Saint-Etienne, Institut d'Optique Graduate School — Laboratoire Hubert Curien, Saint Etienne, France

E-mail: francis.calmon@insa-lyon.fr

Received 18 March 2021, revised 6 May 2021
Accepted for publication 13 May 2021
Published 1 July 2021

Abstract

Single photon avalanche diodes (SPADs) are widely used to monitor fast and weak optical signals. The modeling of two main figures of merit of SPAD, namely the dark count rate (DCR) and the photon detection probability, requires one to calculate the avalanche triggering probability (ATP), usually obtained by numerically solving two transcendental equations (the McIntyre model) as post processing of technology computer-aided design simulations. This paper proposes an analytical alternative to this approach, exploiting an approximation of the impact ionization rates, in principle valid only under high field conditions, but extended to all fields by a simple fitting procedure. The proposed approximated/analytical ATP calculation can be efficient and relevant for SPAD compact modeling that is compatible with a spice-like simulator. As an illustration, a full analytical calculation for DCR based on both ATP and generation terms for a P^+N abrupt diode junction is presented.

Keywords: single photon avalanche diode, avalanche triggering probability, McIntyre model, dark count rate, compact modeling

(Some figures may appear in color only in the online journal)

1. Introduction

Single photon avalanche diodes (SPADs) are essentially PN junctions that are reverse biased above the breakdown voltage that can be used for detection of photons or charged particles. The basic working principle of SPADs (or avalanche diodes operating in the Geiger mode) is that it takes few absorbed photons or the path of charged particles to generate an electron–hole pair, that may reach the multiplication region and trigger an avalanche. Once the avalanche is triggered, a high current circulates through the device and may damage it, if not properly extinguished [1–3]. To avoid degradation, quenching circuits (such as a simple series resistor) are used to turn off the avalanche current. After quenching, the SPAD is set ready for another detection, as illustrated in figure 1.

* Author to whom any correspondence should be addressed.

Original content from this work may be used under the terms of the Creative Commons Attribution 4.0 licence. Any further distribution of this work must maintain attribution to the author(s) and the title of the work, journal citation and DOI.

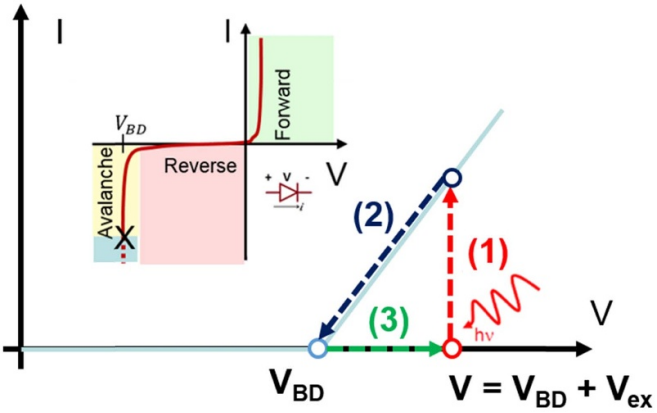

Figure 1. The working principle of Geiger-mode photodiodes. (1) The PN junction is reverse biased above the breakdown voltage (V_{BD}); V_{ex} is the excess voltage. (2) Once a photon hits the SCR and generates an electron–hole pair, the latter is accelerated due to a high electric field and produces a high current, due to ionization impact. (3) Quenching electronics reduce voltage across the diode. The SPAD is then ready for a new detection.

SPADs have been widely used for several applications: detection of weak optical signals, time of flight measurements [4–6] and detection of charged particles [7–9], for example. The main drawback of SPAD devices is their intrinsic noise, called the dark count rate (DCR), corresponding to the number of avalanches that are triggered in dark conditions (false detections) for a fixed time window. Carriers that eventually start the avalanche can be produced by thermal generation, band-to-band (B2B) tunneling or migration into the multiplication zone from the neutral zones [8]. The DCR estimation can be carried out by integrating the product of the generation rate within the space charge region (SCR) by the avalanche triggering probability (ATP), noted as P_p [9–11]. P_p calculation is also needed to estimate the photon detection probability (PDP) and efficiency of the device [12].

To calculate P_p, the McIntyre model [13] has been widely used. It was developed in 1973, based on Oldham's equations [14]. Starting from the ionization coefficients for electrons and holes, it states that one can numerically calculate the probability of avalanche triggering for a carrier at the beginning of the SCR as the multiplication region (holes for an NP junction, and electrons for a PN junction), and then one can determine the total ATP across the SCR. This model has recently been implemented in Synopsys Sentaurus [15]. The main inconvenience of this model lies in the fact that at least two transcendental equations need to be numerically solved, preventing any use in the field of compact modeling. In this paper, an alternative analytical solution is proposed, based on a high electric field approximation. In the next section, the McIntyre model theory is reviewed. In section 3, the new analytical approach principle is presented in detail and comparisons between rigorous and approximated models are presented. In section 4, a practical method for choosing adequate fitting parameters is proposed. The results of DCR calculations are shown in section 5, including a full analytical method, before the conclusions are presented.

2. Theoretical background

The model of Oldham [14] and McIntyre [13] is a powerful technique used to compute the joint probability $P_p(x)$, i.e. the probability that an electron–hole pair generated at x will initiate an avalanche in the space charge layer of an NP junction. Once P_p is known, it is possible to deduce the DCR or PDP, two SPAD figures of merit, by means of post processing analysis of technology computer-aided design (TCAD) simulations.

Let us provide a recap of the main results of this model. The joint (electron and hole) ATP P_p is given by:

$$P_p(x) = \frac{P_h(0) f(x)}{1 - P_h(0) + P_h(0) f(x)} \tag{1}$$

where $P_h(x)$ is the probability that an avalanche will be initiated by a hole that has been generated at position x, i.e. $P_h(0)$ represents the probability that a hole triggers an avalanche at the edge of the left-side N-doped region (boundary condition), and $f(x)$ is given by:

$$f(x) = \exp\left(\int_0^x (\alpha_e(u) - \alpha_h(u))\,du\right) \tag{2}$$

where α_e and α_h are the electron and hole ionization rates, respectively.

The boundary condition $P_h(0)$ can be found by solving the following transcendental equation:

$$1 = (1 - P_h(0))\,\exp\left[\int_0^W \frac{\alpha_h(u) P_h(0) f(u)}{1 - P_h(0) + P_h(0) f(u)}\,du\right] \tag{3}$$

Despite its simplicity, the model requires several numerical calculations, essentially because the integral equations (2) and (3) do not have any closed form solution, limiting its use in the field of compact modeling. Indeed, the various analytical equations of the ionization coefficient, α_e (for electrons) and α_h (for holes) that have been proposed in the literature [16–19], cannot be analytically integrated. Actually, as an example, the ionization coefficient function of the electric field E can be formulated with the Okuto–Crowell equation [17] as follows:

$$\alpha_{OC}(E) = aE \exp\left(-\frac{b}{E^2}\right) \tag{4}$$

or the Reggiani model (also known as the UniBo model) [19] by:

$$\alpha_R(E) = \frac{E}{a + b\exp\left[\frac{d}{E+c}\right]} \tag{5}$$

where a, b, c, d are model parameters.

In this paper, an approximated method is proposed to address this issue.

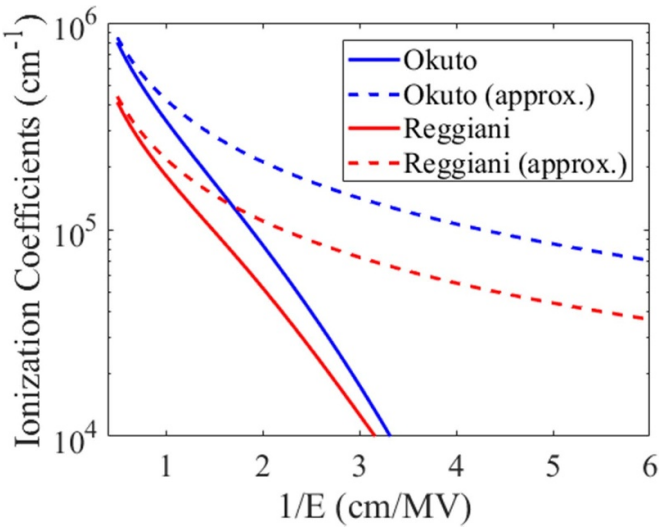

Figure 2. The electron impact ionization coefficient versus the inverse of the electric field at $T = 323$ K, for Okuto–Crowell and Reggiani equations. Original model: solid line; approximation: dotted line.

3. A novel approach for ATP P_p analytical estimation

3.1. Presentation of the model: main approximation

Let us first observe that under high electric field conditions ($E >$ few 100 kV cm^{-1}), all models predict a linear dependency of the ionization coefficient on the electric field, as can be seen in figure 2

$$\alpha_{\mathrm{OC}}(E) \underset{E\to\infty}{\to} aE \tag{6}$$

$$\alpha_{\mathrm{R}}(E) \underset{E\to\infty}{\to} \frac{E}{a+b} \tag{7}$$

Interestingly, it may be convenient to use such an approximation, as the electric field E can easily be integrated, observing that:

$$\int_0^x E(x)\,\mathrm{d}x = \int_{V(0)}^{V(x)} -\mathrm{d}V = V(0) - V(x) \tag{8}$$

However, the high field approximation of the ionization coefficient is typically valid in a limited range, close to the maximum of the electric field profile, and not in the full space charge layer, where, in contrast, the ionization coefficient becomes rapidly negligible.

Starting from these observations, the central idea of this paper consists of using the following linear approximation (β coefficient) for the ionization coefficient in a limited area of the space charge layer, figure 3

$$\text{For } x_a < x < x_b, \qquad \alpha(E) = \beta E \tag{9}$$

$$\text{For } x < x_a \text{ or } x > x_b, \qquad \alpha(E) = 0 \tag{10}$$

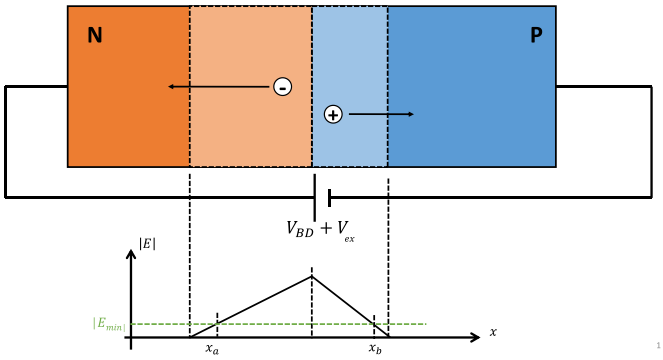

Figure 3. A schematic drawing of the electric field in an NP junction (abrupt junction approximation), indicating x_a and x_b abscissas.

The abscissas x_a and x_b are defined from a minimum value $E_{\min}$ of the electric field (as illustrated in figure 3). When $E < E_{\min}$, the ionization coefficients for electrons and holes are assumed negligible

$$E(x_a) = E(x_b) = E_{\min} \tag{11}$$

The values of β (β_{e} for electrons and β_{h} for holes) can be taken from their extremum values in high field conditions, respectively, for Okuto–Crowell and Reggiani models:

$$\beta_{\mathrm{HF\,OC}} = a \tag{12}$$

$$\beta_{\mathrm{HF\,R}} = \frac{1}{a+b} \tag{13}$$

To account for eventual deviation to the high field approximation (a real SPAD typically operates in moderate electric fields to prevent B2B tunneling and, consequently, excessive DCRs), a fitting parameter γ has been introduced for electrons and holes. The values of the fitting parameters γ depend on the value of the maximum electric field in the structure, which is directly related to the applied voltage across the junction. A discussion on how to choose the fitting parameters for this model is presented in section 4

$$\beta = \frac{\beta_{\mathrm{HF}}}{\gamma} \tag{14}$$

According to this approximation,

$$\alpha_{\mathrm{e,h}}(x) = \beta_{\mathrm{e,h}} E(x) \text{ if } x_a < x < x_b \tag{15}$$

3.2. Application to the calculation of the avalanche triggering probabilities for electrons and holes (P_e and P_h)

Using equation (15), the $f(x)$ function can be calculated as:

$$f(x) = \exp\left(\int_0^x (\alpha_{\mathrm{e}}(u) - \alpha_{\mathrm{h}}(u))\,\mathrm{d}u\right) = \exp\left(\int_{V(x_a)}^{V(x)} -(\beta_{\mathrm{e}} - \beta_{\mathrm{h}})\,\mathrm{d}V\right) \tag{16}$$

$$f(x) = \exp\left(\left(\beta_e - \beta_h\right)\left(V(x_a) - V(x)\right)\right), \text{ for } x_a < x < x_b \quad (17)$$

$$f(x) = \exp\left(\left(\beta_e - \beta_h\right)\left(V(x_a) - V(x_b)\right)\right), \text{ for } x > x_b \quad (18)$$

$P_h(x)$ is the probability that an avalanche will be initiated by a hole that has been generated at position x. The probability $P_h(x)$ can be calculated as follows [13].

For $x_a < x < x_b$:

$$P_h(x) = 1 - (1 - P_h(0))\ \exp\left[\int_0^x \alpha_h(u) P_p(u)\ \mathrm{d}u\right] \quad (19)$$

Let us introduce the quantity $I(x)$ as:

$$I(x) = \int_0^x \alpha_h(u) P_p(u)\ \mathrm{d}u = \int_0^x \frac{\alpha_h(u) P_h(0) f(u)}{1 - P_h(0) + P_h(0) f(u)}\ \mathrm{d}u \quad (20)$$

By using the proposed approximation, $I(x)$ can be integrated, leading to:

$$I(x) = \int_{x_a}^{x} \frac{\beta_h E(u) P_h(0) \exp\left(\left(\beta_e - \beta_h\right)\left(V(x_a) - V(u)\right)\right)}{1 - P_h(0) + P_h(0) \exp\left(\left(\beta_e - \beta_h\right)\left(V(x_a) - V(u)\right)\right)}\ \mathrm{d}u \quad (21)$$

$$I(x) = \int_{V(x_a)}^{V(x)} \frac{-\beta_h P_h(0) \exp\left(\left(\beta_e - \beta_h\right)\left(V(x_a) - V\right)\right)}{1 - P_h(0) + P_h(0) \exp\left(\left(\beta_e - \beta_h\right)\left(V(x_a) - V\right)\right)}\ \mathrm{d}V \quad (22)$$

$$I(x) = \frac{\beta_h}{\beta_e - \beta_h}\left[\ln\left(1 - P_h(0) + P_h(0) \exp\left(\left(\beta_e - \beta_h\right)\right.\right.\right. \times \left.\left.\left.\left(V(x_a) - V\right)\right)\right)\right]_{V(x_a)}^{V(x)} \quad (23)$$

$$I(x) = \frac{\beta_h}{\beta_e - \beta_h} \ln\left[1 - P_h(0) + P_h(0) \exp\left(\left(\beta_e - \beta_h\right)\right.\right. \times \left.\left.\left(V(x_a) - V(x)\right)\right)\right] \quad (24)$$

$$P_h(x) = 1 - (1 - P_h(0))\ (1 - P_h(0) + P_h(0) \exp\left(\left(\beta_e - \beta_h\right)\right. \times \left.\left(V(x_a) - V(x)\right)\right))^{\frac{\beta_h}{\beta_e - \beta_h}} \quad (25)$$

For $> x_b$:

$$P_h(x) = 1 - (1 - P_h(0))\ (1 - P_h(0) + P_h(0) \exp\left(\left(\beta_e - \beta_h\right)\right. \times \left.\left(V(x_a) - V(x_b)\right)\right))^{\frac{\beta_h}{\beta_e - \beta_h}} \quad (26)$$

$P_h(0)$ is an unknown boundary condition, the solution of the following transcendental equation:

$$0 = 1 - (1 - P_h(0))\ (1 - P_h(0) + P_h(0) \exp\left(\left(\beta_e - \beta_h\right)\right. \times \left.\left(V(x_a) - V(x_b)\right)\right))^{\frac{\beta_h}{\beta_e - \beta_h}} \quad (27)$$

This equation can be rewritten as (for $P_h(0 \neq 1)$):

$$\frac{1}{(1 - P_h(0))} = (1 - P_h(0) + P_h(0) \exp\left(\left(\beta_e - \beta_h\right)\right. \times \left.\left(V(x_a) - V(x_b)\right)\right))^{\frac{\beta_h}{\beta_e - \beta_h}} \quad (28)$$

$P_e(x)$ is the probability that an avalanche will be initiated by an electron that has been generated at position x. Similarly, the probability $P_e(x)$ can be calculated starting from:

$$P_e(x) = 1 - \exp\left(\int_0^x \alpha_e P_p(x)\,\mathrm{d}x\right) \quad (29)$$

Leading to, for $x < x_b$:

$$P_e(x) = 1 - (1 - P_h(0) + P_h(0) \exp\left(\left(\beta_e - \beta_h\right)\right. \times \left.\left(V(x_a) - V(x)\right)\right))^{\frac{\beta_e}{\beta_e - \beta_h}}. \quad (30)$$

And for $x > x_b$:

$$P_e(x) = 1 - (1 - P_h(0) + P_h(0) \exp\left(\left(\beta_e - \beta_h\right)\right. \times \left.\left(V(x_a) - V(x_b)\right)\right))^{\frac{\beta_e}{\beta_e - \beta_h}} \quad (31)$$

Equations (25) and (26) are analytical expressions for $P_h(x)$ (and for $P_e(x)$, respectively, equations (30) and (31)), provided that $P_h(0)$ is extracted from a numerical solution of equation (28), and that the fitting parameters γ_e and γ_h have been found. These results are compared with TCAD simulations in the next section.

3.3. Comparisons with TCAD simulations

To validate the model and its assumptions, comparisons have been performed with TCAD simulations (Synopsys) under several conditions: textbook NP abrupt junctions with uniform doping profiles (both symmetrical, i.e. the same N and P doping level or asymmetrical), and more realistic non-uniform doping profile PN junctions. In all cases, the popular Okuto–Crowell impact ionization model has been used (although tests

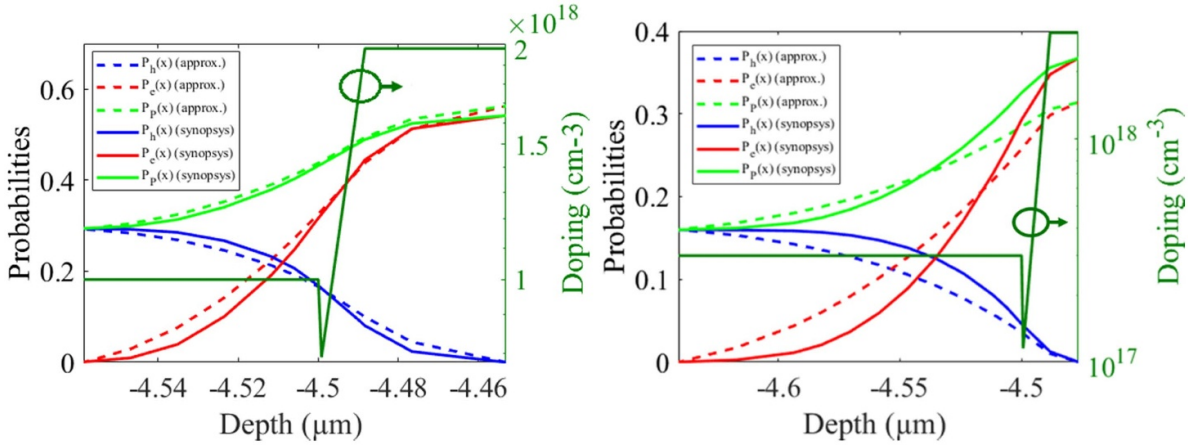

Figure 4. Avalanche triggering probabilities for electrons, holes and pair in an abrupt NP junction. Synopsys simulations (McIntyre model) are the solid line, and the model proposed here is the dotted line. The doping profile is also indicated in log scale. The excess voltage is 1 V. Figure 4-left: an almost symmetrical N^+P^+ junction ($V_{BD} = 5.3$ V and $\gamma_e = 2.25$, $\gamma_h = 2.77$). Figure 4-right: an asymmetrical NP^+ junction ($V_{BD} = 7.1$ V and $\gamma_e = 1.54$, $\gamma_h = 2.10$).

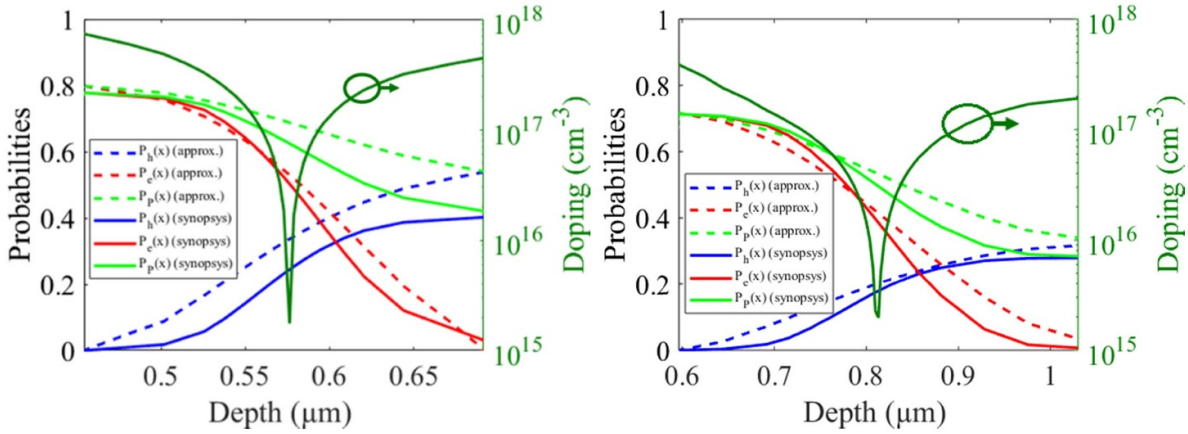

Figure 5. Avalanche triggering probabilities for electrons, holes and pair in a non-abrupt PN junction [11]. Synopsys simulations (McIntyre model) are the solid line, and the model proposed here is the dotted line. The doping profile is also indicated in log scale. The excess voltage is 2 V. Figure 5-left: a PN junction with equivalent doping level on both sides ($V_{BD} = 9.5$ V and $\gamma_e = 1.54$, $\gamma_h = 2.10$). Figure 5-right: a less abrupt PN junction ($V_{BD} = 16$ V and $\gamma_e = 3.30$, $\gamma_h = 6.05$).

(not shown here) have also been performed with the Reggiani model, leading to similar conclusions).

In the model, the threshold for ionization has been set to $E_{min} = 0.1$ MV cm^{-1} for both electrons and holes (i.e. the default threshold electric field for the definition of the multiplication region used in the Sentaurus device simulator [15]), and the fitting parameters γ have been set by adjusting the function $f(x)$ (equation (2)) numerically and analytically calculated using equations (17) and (18). An alternative approach for determining γ is proposed in section 4.

All the results (see figure 4 for an abrupt NP junction and figure 5 for a non-abrupt PN junction [11]) indicate an overall good agreement between simulations and the model, demonstrating its capability of capturing the correct trend for ionization probabilities, even in cases where the high field conditions are not satisfied. As expected, the fitting parameters γ tend to increase when the electric field within the space charge layer decreases, as in the case of low excess voltage or non-abrupt junctions.

4. Determination '*a priori*' of the γ fitting parameters

As seen in section 3, the good choice of fitting parameters γ is crucial to improve the model accuracy. So far, the γ parameters have been obtained by fitting the exact solution of equation (2) using its approximation (equation (16)). This procedure is quite simple, and has been found to be quite efficient in all devices tested. However, it needs to be done for each voltage and each doping profile.

In the following, an empirical procedure is proposed to determine a reasonable value of γ, avoiding this calibration procedure.

To this aim, two abrupt NP junctions were analyzed by means of TCAD simulations. The first is a symmetrical abrupt junction, while the second is asymmetrical. Their doping concentrations can be seen in table 1. For both junctions, the applied reverse voltage ($V_{BD} + V_{ex}$) was varied, aiming to change the value of the electric field. Then, the fitting parameters were manually adjusted to provide a good

Table 1. Doping parameters for symmetrical and asymmetrical abrupt junctions.

	N_D (cm^{-3})	N_A (cm^{-3})
Asymmetrical junction	2×10^{18}	3×10^{18}
Symmetrical junction	3×10^{18}	3.3×10^{18}

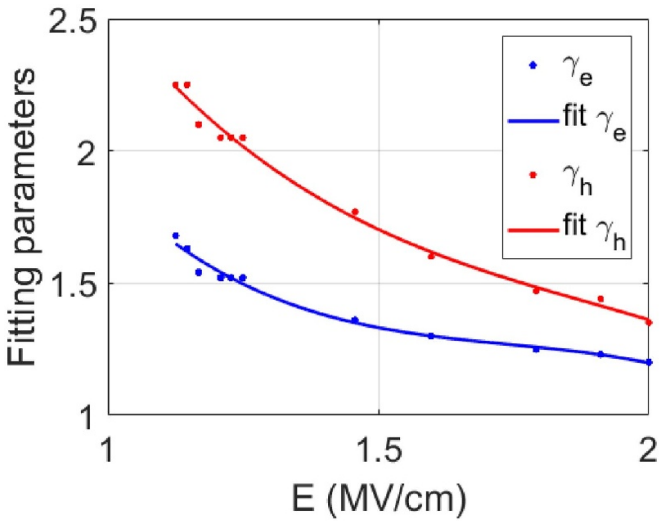

Figure 6. Fitting parameters for electrons and holes in the symmetrical abrupt junction.

approximation of the probabilities (maximum error = 10%, when compared to TCAD results). It is possible to observe that the fitting parameters highly depend on the maximum value of the electric field in the junction (figures 6 and 7); this value is basically a function of the applied voltage and doping parameters. By considering that the latter is often not precisely known in commercial technologies, due to confidentiality issues, this paper focuses on determining γ according to the applied reverse voltage ($V_{BD} + V_{ex}$).

The evolution of these fitting parameters according to the maximum of the electric field is plotted in figures 6 and 7. As can be seen, both γ_e and γ_h follow a 3rd order polynomial evolution, according to excess bias voltage:

$$\gamma(V_{ex}) = aV_{ex}^3 + bV_{ex}^2 + cV_{ex} + d \tag{32}$$

where a, b, c, d are fitting coefficients.

The coefficients that describe the curves in figures 6 and 7 can be seen in table 2. By taking into account the nature of the junction's doping (symmetrical or asymmetrical), and by knowing the excess voltage applied to the junction, one can determine the fitting parameters for the model, by using the aforementioned curves.

5. Implementation of the analytical solution of the ATP for the DCR estimation

To estimate the DCR (only taking into account the contribution of the SCR), equation (33) is often used [9–11, 20, 21], where

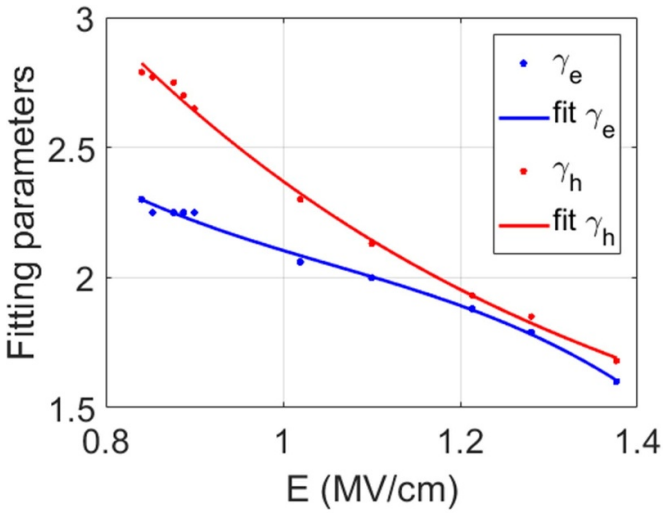

Figure 7. Fitting parameters for electrons and holes in the asymmetrical abrupt junction.

Table 2. Coefficients used in equation (32) to describe the fitting parameters' evolution according to excess voltage applied to the junction.

	Symmetrical junction		Asymmetrical junction	
	γ_e	γ_h	γ_e	γ_h
a	−1.106	−0.822	−3.7	−1.028
b	5.777	4.664	11.72	5.243
c	−10.26	−9.406	−13.37	−9.874
d	7.453	8.092	7.454	8.03

$P_p(x)$ is the ATP and GR(x) is the carriers' generation rate in the SCR (1D approach)

$$\mathrm{DCR} = \int_{x_a}^{x_b} P_p(x)\ \mathrm{GR}(x)\ \mathrm{d}x \tag{33}$$

When calculating the DCR from equation (33), the generation rate can be obtained by TCAD simulations, when considering Shockley–Read–Hall (SRH) accounting for trap-assisted tunneling (TAT) contribution and B2B generation–recombination mechanisms, or the B2B tunneling effect alone, for example. As an illustration, we present, in figure 8, the DCR estimation based on both the rigorous and approximated/analytical ATP calculation (here, the SRH and B2B generation rates were obtained by TCAD simulations). As observed in figure 8, differences are negligible, which validates the use of the P_p analytical model to estimate the DCR in SPAD devices.

The proposed approximated/analytical ATP calculation can be efficient and relevant when considering a full analytical calculation that includes generation rates. Hence, the GR(x) term can also be analytically formulated for compact modeling purposes [20, 21]. As a first assumption, GR(x) can be estimated as the sum of the SRH and B2B generation processes.

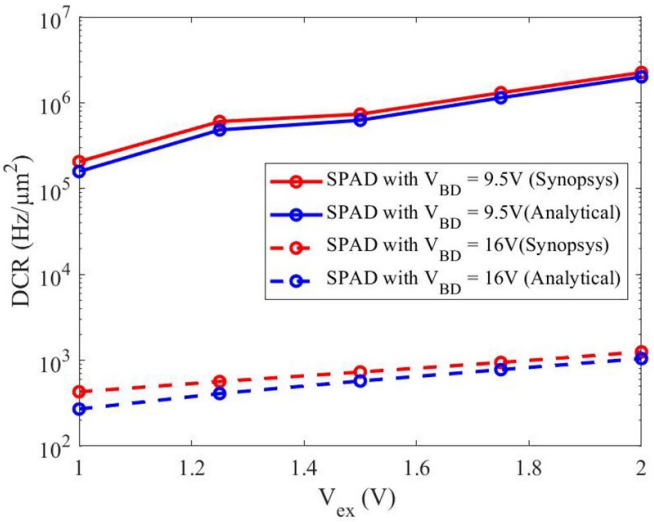

Figure 8. Estimation of the DCR as a function of excess voltage for the same devices as in figure 5 with a non-abrupt PN junction. The generation rates were obtained by TCAD simulations, while changing the ATP calculation method (rigorous or approximate/analytical).

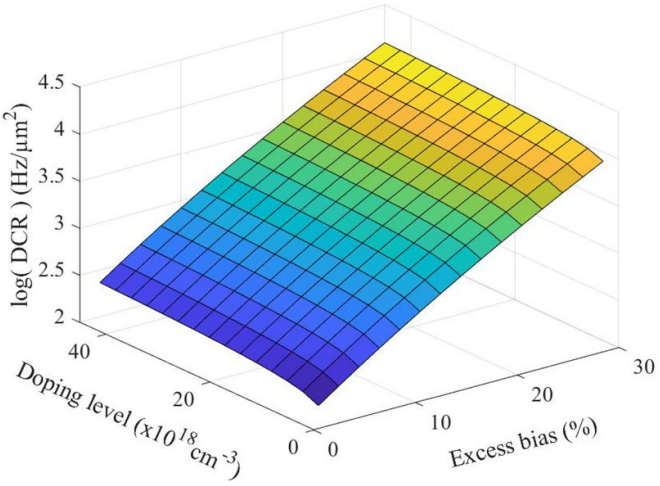

Figure 9. DCR estimation based on full analytical formulation for the ATP and generation terms (P^+N abrupt diode junction) function of excess bias and P^+ doping level ($N_D = 3 \times 10^{17}$ cm^{-3}, $T = 300$ K).

Concerning the SRH generation process in the SCR, a preliminary formulation can be expressed as $GR^{SRH} = \frac{n_i}{\tau_n + \tau_p}$, where τ_n and τ_p are the carrier lifetimes for electrons and holes, respectively. These can be formulated as the function of the doping level (N_{doping}), the temperature (T) and the electric field (E) using the following equation [15, 20, 21]

$$\tau = \left(\tau_{min} + \frac{\tau_{max} - \tau_{min}}{1 + \left(\frac{N_{doping}}{N_{REF}}\right)^{\beta}}\right)\left(\frac{T}{300}\right)^{\alpha}\left(1 + \Gamma_{TAT}(E)\right)^{-1} \tag{34}$$

where $\tau_{min}, \tau_{max}, N_{REF}, \alpha, \beta$ are the carrier lifetime model parameters (depending on whether we consider electrons or holes). Here, $(1 + \Gamma_{TAT}(E))^{-1}$ is a correction term accounting for the TAT effect. The $\Gamma_{TAT}(E)$ function can be expressed as Hurkx *et al* or Schenk *et al* proposals as described and implemented in [15].

A $\Gamma_{TAT}(E)$ compact formulation has also been proposed by Hurkx *et al* [22] and is used in Xu *et al's* work [20, 21]:

$$\Gamma_{TAT}(E) = 2\sqrt{3\pi}\frac{|E|}{E_\Gamma}\exp\left[\left(\frac{E}{E_\Gamma}\right)^2\right] \text{ with } E_\Gamma = \frac{\sqrt{24m^*(kT)^3}}{q\hbar} \tag{35}$$

where m^* is the effective mass of the carrier ($m^* = 0.25\,m_0$, with m_0 the free electron rest mass), and k and $\hbar$ are, respectively, the Boltzmann and the reduced Planck constants.

On the other hand, the B2B generation (GR^{B2B}) can be expressed following various models. As an example, one can use Liou formulation [23] for the GR^{B2B} function of the electric field (E), available in [15] as follows:

$$GR^{B2B} = A \cdot |E|^B \cdot \exp\left(-\frac{C}{|E|}\right) \tag{36}$$

Table 3. The main parameters used in equations (34)–(36).

Category	Parameter	Value	Unit
SRH model (equation (34)) and (equation (35))	τ_{min} (electron/hole)	$10^{-4}/3 \times 10^{-5}$	μs
	τ_{max} (electron/hole)	$10^{-3}/3 \times 10^{-4}$	μs
	N_{doping}	10^{16}	cm^{-3}
	α	1	—
	β	1	—
	m^*/m_0	0.25	—
Band-to-band model (equation (36))	A	1.1×10^{27}	cm^{-2} s^{-1} V^{-1}
	B	1.8	—
	C	21.3×10^6	V cm^{-1}

where A, B, C are the B2B generation model parameters.

As an illustration of a full analytical calculation for both ATP and generation terms, figure 9 presents the DCR estimation for a P^+N abrupt diode junction function of excess bias and P^+ doping level (parameter details are shown in table 3). This efficient approach allows one to retrieve the DCR increase with excess bias voltage and doping level taking into account the B2B generation and ATP dependence on biasing conditions and electrical field distribution (linked to the doping level). In this specific case, the TAT effects are negligible compared to the B2B contribution. However, note that as this model essentially focuses on the modeling of the ATP $P_p(x)$, it is valid no matter which model is used for the generation rate. This aims to implement a full analytical approach for SPAD compact modeling that is compatible with a spice-like simulator (e.g. the Verilog-A model), where the DCR value can be used to generate events with the inter-avalanche time t_a expressed as $t_a = -\frac{1}{DCR} \cdot \ln(1 - \text{random}[0 \ldots 1])$, i.e. the Poisson distribution.

6. Conclusion

In this paper, an analytical approach was proposed to calculate avalanche triggering probabilities in SPADs. This method consists of using high electric field approximation for ionization coefficients, which lead to a closed form solution of McIntyre's equations. This method can be extended to the average and low-field regime, provided that one fitting parameter for the electron and one for the hole are introduced. In this latter case, the accuracy of the approximation depends on the choice of fitting parameters, which depend essentially on the maximum value of the electrical field in the multiplication region, and thus on the doping profile and applied voltage. These fitting parameters can be either found accurately using case-to-case study, or qualitatively, using empirical laws, calibrated on symmetrical and asymmetrical abrupt NP junctions. The proposed approximation provides faster results than the method implemented in TCAD simulation, allowing one to calculate the DCR for instance with very good accuracy.

Data availability statement

The data that support the findings of this study are available upon reasonable request from the authors.

Acknowledgments

The authors would like to thank the following for funding: the Auvergne Rhone Alpes region (ARC6 Research Program 2016 No. 16-005689-01), the French National Research Agency (ANR-18-CE24-0010), the Nano2022 research program.

ORCID iD

Francis Calmon https://orcid.org/0000-0001-5076-076X

References

[1] Dalla Betta G-F, Pancheri L, Stoppa D, Henderson R and Richardson J 2011 *Advances in Photodiodes: Avalanche Photodiodes in Submicron CMOS Technologies for High-Sensitivity Imaging* ed G-F Dalla Betta (London: IntechOpen) pp 225–48

[2] Charbon E, Fishburn M, Walker R, Henderson R K and Niclass C 2013 *SPAD-Based Sensors. TOF Range-Imaging Cameras* (Berlin: Springer) pp 11–38

[3] Cova S, Ghioni M, Itzler M A, Bienfang J C and Restelli A 2013 Semiconductor-based detectors. Single-photon generation and detection. Physics and applications *Exp. Methods Phys. Sci.* **45** 83–146

[4] Niclass C, Soga M, Matsubara H and Kato S 2011 A 100 m-range 10-frame/s 340 × 96-pixel time-of-flight depth sensor in 0.18 μm CMOS *Proc. ESSCIRC* pp 107–10

[5] Henderson R K, Johnston N, Mattioli Della Rocca F, Chen H, Day-Uei Li D, Hungerford G, Hirsch R, McLoskey D, Yip P and Birch D J S 2019 A 192 × 128 time correlated SPAD image sensor in 40-nm CMOS technology *IEEE J. Solid-State Circuits* **54** 1907–16

[6] Ruokamo H, Hallman L W and Kostamovaara J 2019 An 80 × 25 pixel CMOS single-photon sensor with flexible on-chip time gating of 40 subarrays for solid-state 3D range imaging *IEEE J. Solid-State Circuits* **54** 501–10

[7] Vilella E and Diéguez A 2012 A gated single-photon avalanche diode array fabricated in a conventional CMOS process for triggered systems *Sens. Actuators* A **186** 163–8

[8] Pancheri L, Brogi P, Collazuol G, Dalla Betta G-F, Ficorella A, Marrocchesi P S, Morsani F, Ratti L and Savoy-Navarro A 2017 First prototypes of two-tier avalanche pixel sensors for particle detection *Nucl. Instrum. Methods Phys. Res.* A **845** 143–6

[9] Vignetti M M *et al* 2018 3D silicon coincidence avalanche detector (3D-SiCAD) for charged particle detection *Nucl. Instrum. Methods Phys. Res.* A **881** 53–9

[10] Vignetti M M, Calmon F, Lesieur P and Savoy-Navarro A 2017 Simulation study of a novel 3D SPAD pixel in an advanced FD-SOI technology *Solid State Electron.* **128** 163–71

[11] Chaves de Albuquerque T, Calmon F, Clerc R, Pittet P, Benhammou Y, Golanski D, Jouan S, Rideau D and Cathelin A 2018 Integration of SPAD in 28 nm FDSOI CMOS technology *2018 48th European Solid-State Device Research Conf. (ESSDERC) (Dresden)* pp 82–5

[12] Renker D and Lorenz E 2009 Advances in solid state photon detectors *J. Instrum.* **4** P04004

[13] McIntyre R J 1973 On the avalanche initiation probability of avalanche diodes above the breakdown voltage *IEEE Trans. Electron Devices* **20** 637–41

[14] Oldham W G, Samuelson R R and Antognetti P 1972 Triggering phenomena in avalanche diodes *IEEE Trans. Electron Devices* **19** 1056–60

[15] Synopsys 2018 Sentaurus Device User Guide Version O-2018.06

[16] van Overstraeten R and de Man H 1970 Measurement of the ionization rates in diffused silicon p–n junctions *Solid State Electron.* **13** 583–608

[17] Okuto Y and Crowell C R 1975 Threshold energy effect on avalanche breakdown voltage in semiconductor junctions *Solid State Electron.* **18** 161–8

[18] Lackner T 1991 Avalanche multiplication in semiconductors: a modification of Chynoweth's law *Solid State Electron.* **34** 33–42

[19] Reggiani S *et al* 2005 Measurement and modeling of the electron impact-ionization coefficient in silicon up to very high temperatures *IEEE Trans. Electron Devices* **52** 2290–9

[20] Xu Y, Xiang P and Xie X 2017 Comprehensive understanding of dark count mechanisms of single-photon avalanche diodes fabricated in deep sub-micron CMOS technologies *Solid State Electron.* **129** 168–74

[21] Xu Y, Xiang P, Xie X and Huang Y 2016 A new modeling and simulation method for important statistical performance prediction of single photon avalanche diode detectors *Semicond. Sci. Technol.* **31** 065024

[22] Hurkx G A M, Klaassen D B M and Knuvers M P G 1992 A new recombination model for device simulation including tunneling *IEEE Trans. Electron Devices* **39** 331–8

[23] Liou J J 1990 Modeling the tunnelling current in reverse-biased p/n junctions *Solid State Electron.* **33** 971–2